Supporting Information

Ballottari et al. 10.1073/pnas.1404377111

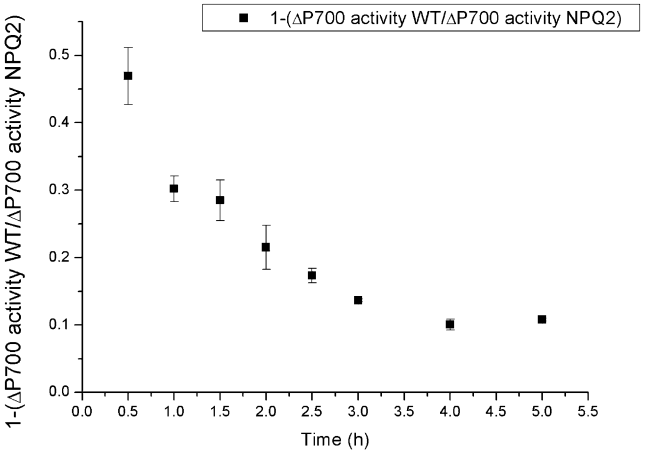

Fig. S1. Effect of zeaxanthin photoprotection in isolated photosystem I (PSI)–light-harvesting complex I (LHCI) complexes. PSI–LHCI complexes from WT and nonphotochemical quenching 2 (*npq2*) mutants were subjected to photooxidative stress as described in Fig. 1. The fraction of P700 activity that is preserved because of zeaxanthin photoprotection was calculated as 1 minus the ratio between the changes in P700 activity in the WT and in the *npq2* mutant at the different time points.

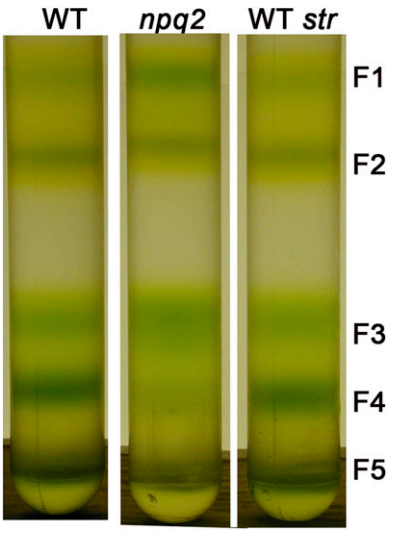

Fig. S2. Separation of PSI–LHCI components by ultracentrifugation. PSI–LHCI from WT, *npq2* mutant, and WT stressed for 30 min at 1,000 μmol·m^{-2}·s^{-1}) (WT str) were solubilized with 0.8% β-dodecyl-maltoside and 0.5% Zwittergent to detach LHCI from PSI-core. Solubilized PSI–LCI was loaded on the sucrose gradient and ultracentrifuged overnight. Fractions recovered are indicated as F1–F5.

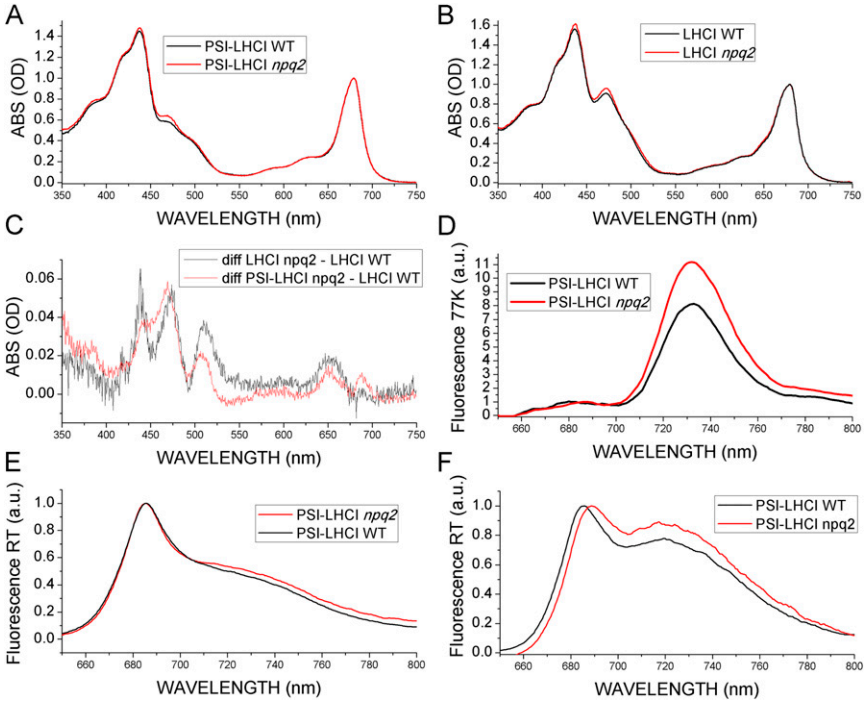

Fig. S3. Spectroscopic characterization of PSI–LHCI and LHCI fractions. (*A* and *B*) Absorption spectra in the visible region of PSI–LHCI (*A*) and LHCI (*B*) isolated from WT and *npq2* leaves. (*C*) Differences in absorption spectra were calculated by subtracting LHCI-WT from LHCI-*npq2* (black line) and PSI–LHCI WT from PSI–LHCI-*npq2* (red line). (*D*–*F*) Fluorescence emission spectra in the 600- to 800-nm region of isolated PSI–LHCI (*D* and *E*) and LHCI (*F*). In *D* fluorescence emission was measured at 77 K.

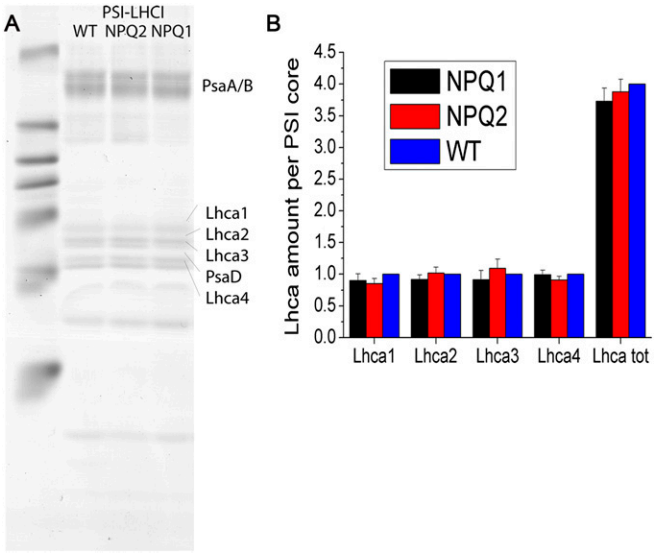

Fig. S4. SDS/PAGE of isolated PSI–LHCI complexes. (*A*) PSI–LHCI complexes isolated from WT and nonphotochemical quenching 1 (*npq1*), *npq2* mutants were loaded on SDS/PAGE denaturing gel stained with Coomassie dye. Photosystem I subunit A/B (PsaA/B), photosystem I subunit D (PsaD), and photosystem I light harvesting complexes 1-4 (Lhca1-4) bands are indicated. The amount of Coomassie bound by each visible band was determined by densitometric analysis with GelPRo software. (*B*) The ratio between Lhca1-4 and PsaD optical density. Lhca tot, sum of the optical density measured for Lhca1–4.

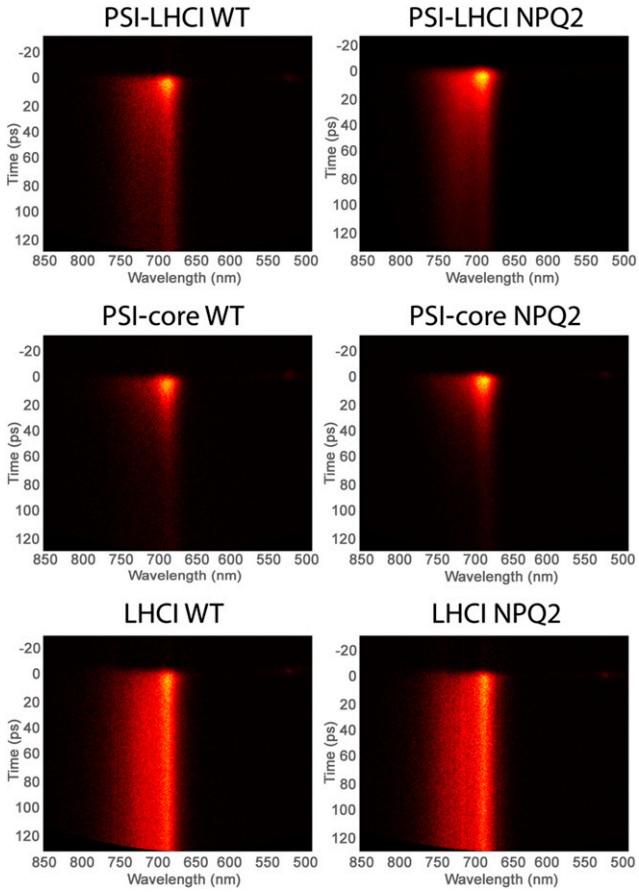

Fig. S5. Streak camera imaging of fluorescence decay of PSI–LHCI, PSI-core, and LHCI. Streak camera imaging was used to measure fluorescence decay of PSI–LHCI, PSI-core, and LHCI samples isolated from WT and *npq2* mutant. Excitation was performed at 440 nm.

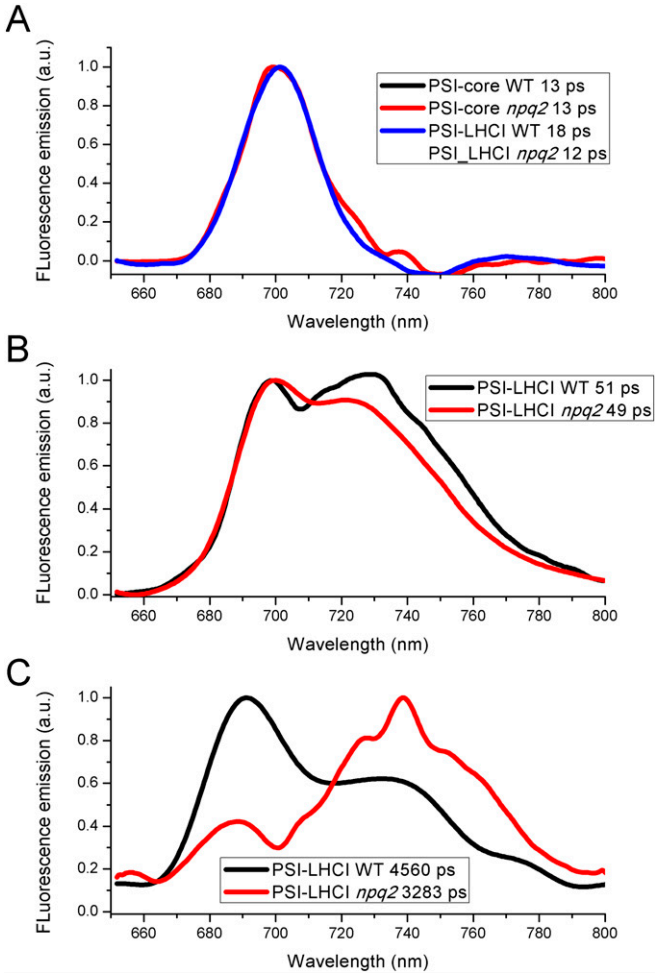

Fig. S6. Decay-associated spectrum of PSI–LHCI WT and *npq2*. Decay-associated spectra reported in Fig. 4 were normalized to the maximum value. (*A*) Comparison of 12- to 18-ps components of WT and *npq2* PSI-core and PSI–LHCI samples. (*B*) Comparison of 49- and 51-ps components of PSI–LHCI WT and *npq2*. (*C*) Comparison of the longest decay components calculated in PSI–LHCI WT and *npq2*.

Table S1. Pigment composition of isolated PSI–LHCI

	Chl total	Chl a and b	Chl a	Chl b	Chl/car	Car total	Neo	Viola	Antera	Lute	Zea	β-Car	D.I.	Zea/car total
PSI–LHCI WT	165	6.64	143.41	21.59	4.95	33.33	0.00	3.63	0.00	8.49	0.00	21.21	0.00	0.00
PSI–LHCI *npq2*	165	6.25	142.23	22.77	5.02	32.88	0.00	0.00	0.00	5.97	5.40	21.51	1.00	0.16
PSI–LHCI WT stress	165	7.44	145.45	19.55	5.06	32.63	0.00	2.82	0.56	8.55	0.88	19.82	0.27	0.03

Pigment composition of isolated PSI–LHCI complexes analyzed by HPLC. The de-epoxidation index (D.I.) was calculated as (zea + 0.5*antera)/(zea+antera+viola). The total chlorophyll number was set to 165 according to ref. 1. antera, anteraxanthin; β-car, β-carotene; car, carotenoids; chl, chlorophyll; lute, lutein; neo, neoxanthin; viola, violaxanthin; zea, zeaxanthin. Relative SDs are <5% for all samples ($n = 3$).

1. Ben-Shem A, Frolow F, Nelson N (2003) Crystal structure of plant photosystem I. *Nature* 426(6967):630–635.

Table S2. Pigment composition of sucrose gradient fractions obtained after PSI–LHCI solubilization

	Chl total	Chl a and b	Chl a	Chl b	Chl /Car	Car total	Neo	Viola	Antera	Lute	Zea	β-Car	D.I.	Zea/car total	Chl distribution, %	Viola, %	Zea, %
WT f1	100.00	4.33	81.23	18.77	2.97	33.63	0.00	6.23	0.00	14.19	0.00	13.21	0.00	0.00	6.77	25	0
WT f2	100.00	3.15	75.91	24.09	4.78	20.93	0.00	4.77	0.00	11.03	0.00	5.12	0.00	0.00	15.39	43	0
WT f3	100.00	22.54	95.75	4.25	6.45	15.51	0.00	0.27	0.00	0.34	0.00	14.90	0.00	0.00	9.25	1	0
WT f4	100.00	12.79	92.75	7.25	5.66	17.68	0.00	0.78	0.00	1.87	0.00	15.02	0.00	0.00	26.88	12	0
WT f5	100.00	14.04	93.35	6.65	5.59	17.89	0.00	0.73	0.00	1.62	0.00	15.53	0.00	0.00	41.71	18	0
npq2 f1	100.00	3.38	77.19	22.81	3.38	29.57	0.00	0.00	0.00	8.92	7.31	13.34	1.00	24.73	13.68	0	37
npq2 f2	100.00	2.93	74.53	25.47	5.04	19.86	0.00	0.00	0.00	7.15	6.95	5.76	1.00	35.02	16.94	0	44
npq2 f3	100.00	13.48	93.09	6.91	6.51	15.35	0.00	0.00	0.00	0.68	0.67	14.01	1.00	4.34	18.11	0	5
npq2 f4	100.00	10.26	91.12	8.88	5.89	16.97	0.00	0.00	0.00	1.11	0.91	14.95	1.00	5.37	6.39	0	2
npq2 f5	100.00	13.32	93.02	6.98	7.47	13.39	0.00	0.00	0.00	0.76	0.70	11.94	1.00	5.21	44.88	0	12
WT s f1	100.00	4.87	82.97	17.03	3.01	33.17	0.00	4.87	1.39	13.02	1.66	12.23	0.30	5.00	5.65	15	40
WT s f2	100.00	3.36	77.08	22.92	4.74	21.10	0.00	4.54	0.49	10.35	0.49	5.24	0.13	2.31	14.80	36	31
WT s f3	100.00	23.35	95.89	4.11	7.29	13.73	0.00	0.01	0.00	0.00	0.00	13.73	0.00	0.00	8.61	0	0
WT s f4	100.00	11.16	91.78	8.22	6.89	14.52	0.00	1.08	0.10	2.33	0.11	10.90	0.12	0.77	25.43	15	12
WT s f5	100.00	11.38	91.92	8.08	4.89	20.44	0.00	1.46	0.15	4.82	0.09	13.85	0.90	0.44	45.51	35	17

Pigment composition of fractions f1–5 recovered from sucrose gradient reported in Fig. S2 analyzed by HPLC. Fractions f1–5 resulted from ultracentrifugation in sucrose gradient of solubilized PSI-LHCI purified from dark-adapted WT and npq2 plants, and from WT plants stressed for 30 min at 1,000 $\mu mol \cdot m^{-2} \cdot s^{-1}$ (WT s). Chlorophyll content was set to 100 for all of the samples. WT f1–WT F5 and *npq2* f1– *npq2* f5 represent WT and *npq2* fractions, respectively. The de-epoxidation index (D.I.) was calculated as (zea + 0.5*antera)/(zea+antera+viola). antera, anteraxanthin; β-car, β-carotene; car, carotenoids; Chl, chlorophyll; lute, lutein; neo, neoxanthin; viola, violaxanthin; zea, zeaxanthin. Relative SDs are <5% for all samples ($n = 3$).

Table S3. Pigment composition of recombinant Lhca4 WT and N47H (NH) mutant proteins

	Chl tot	Chl a/b	Chl a	Chl b	Chl /Car	Neo	Viola	Antera	Lute	Zea	Beta-car	Car tot
Lhca4 WT-LV	14	2.62	10.13	3.87	4.40	0.09	0.55	0.00	2.53	0.00	0.00	3.18
Lhca4-WT-LZ	14	2.18	9.60	4.40	4.63	0.01	0.11	0.00	1.68	1.22	0.00	3.02
Lhca4-NH-LV	14	2.54	10.04	3.96	4.74	0.12	0.50	0.00	2.33	0.00	0.00	2.95
Lhca4-NH-LZ	14	2.61	10.13	3.87	5.15	0.02	0.08	0.00	1.52	1.10	0.00	2.72

Recombinant proteins Lhca4 WT and NH mutant were refolded in vitro in the presence of specific pigment mix, obtaining samples binding violaxanthin and lutein (LV) or zeaxanthin and lutein (LZ) in addition to chlorophyll a and b. Pigment compositions of isolated holoproteins analyzed by HPLC are reported in the table. The total number of chlorophyll was set to 14 according to ref. 1. antera, anteraxanthin; β-Car, β-carotene; car, carotenoids; Chl, chlorophyll; lute, lutein; neo, neoxanthin; viola, violaxanthin; zea, zeaxanthin. Relative SDs are <5% for all samples ($n = 3$).

1. Ben-Shem A, Frolow F, Nelson N (2003) Crystal structure of plant photosystem I. *Nature* 426(6967):630–635.

Table S4. Relative fluorescence yield of recombinant Lhca4 holo-proteins ($n = 5$)

Lhca4-WT-LV	SD, %	Lhca4-WT-LZ, %	SD, %	Lhca4-NH-LV, %	SD, %	Lhca4-NH-LZ, %	SD, %
100.0%	3.7	86.3	3.3	133.3	6.5	119.0	6.3

Relative fluorescence quantum yield was determined as normalized fluorescence emission in the 650- to 800-nm region relative to the absorption at the excitation wavelength (625 nm). The value obtained for Lhca4-WT-LV was set at 100%. SDs are indicated ($n = 5$).